MS UMB/2001/107 Revision

NONINVASIVE ASSESSMENT OF VOCAL FOLD MUCOSAL WAVE VELOCITY USING COLOR DOPPLER IMAGING

Yio-Wha Shau[†], Chung-Li Wang[‡],

Fon-Jou Hsieh[‡], Tzu-Yu Hsiao *,

[†] Institute of Applied Mechanics,

National Taiwan University, Taipei, Taiwan.

[‡] Department of Diagnostic Ultrasound

* Department of Otolaryngology;

National Taiwan University Hospital, Taipei, Taiwan

This research was supported by Grant NSC 89-2320-B-002-149 M08

Correspondence and reprint requests to:

Tzu-Yu Hsiao, M.D., Ph.D.

Associate Professor, Department of Otolaryngology,

National Taiwan University Hospital

7, Chung-Sun South Road, Taipei, 10016, Taiwan

TEL: 886-2-23123456 ext. 5214

FAX: 886-2-23410905

E-mail: tzuyu@ha.mc.ntu.edu.tw

Running Title: CDI for Mucosal Wave Velocity

NONINVASIVE ASSESSMENT OF VOCAL FOLD MUCOSAL WAVE VELOCITY USING COLOR DOPPLER IMAGING

ABSTRACT

The vibratory movement of the vocal folds (VF) plays an important role in normal function of phonation. We developed a noninvasive technique to quantify the human MWV *in vivo* using color Doppler imaging (CDI). During phonation the motion of mucosa-air interface generates a unique pattern of US color artifacts which assist the identification of true VF location. An *in vitro* study using vibrating string phantom was conducted to investigate how the CDI displayed a vibrating soft tissue at high frequency. The vibrating amplitude, frequency, mass density and the acoustic impedance of the soft tissues were found to dominate the formation of color artifacts. Based on the model of finite string with fixed ends, we estimated the mean mucosal wave velocity (MWV) for ten adult volunteers (6M 4F, age 34±5) with normal VF function. The mean MWVs for the male subjects were found vary from 2.1 to 10 m/s in frequency range of 85-310 Hz at their comfortable pitch and intensity, while the females typically had higher MWV that varied from 5.0 to 16.5 m/s in frequency range of 180-480 Hz. The MWV increased linearly with the frequency and there was no observable difference in mucosa stiffness due to the effect of gender. The variation in MWV as it propagates vertically can be seen from the color and shape of the artifacts. The VF polyp resulted in abnormal MWV and different CDI vibratory artifacts. The CDI artifacts provide the insight of the dynamics of mucosa structure during phonation, and the method presented is promising for noninvasive monitoring of laryngeal functions clinically.

Keywords: Color Doppler Image, Vocal Fold, Mucosal Wave Velocity, Phonation Function, Ultrasound Artifacts, Laryngeal Ultrasonography

INTRODUCTION

Although clinical ultrasound (US) has been widely used in various noninvasive musculoskelatal diagnoses, its application on the laryngeal examination has been limited due to the spatial resolution and the dynamic response to tiny high frequency movements (Baken and Orlinkoff 2000). The three-dimensional vibratory movements of the vocal folds (VF) are essential for the voice production. Among the basic functions of human larynx, the phonation performance is the most complex and the least well understood activity (Sasaki and Weaver 1997). Therefore, sophisticated noninvasive technologies that combine photoglottography (PGG), electroglottography (EGG) or video laryngostroboscopy with the aerodynamic theories have been developed to investigate the laryngeal function and the neurophysiology of phonation (Hirano 1981; Hanson et al. 1995; Lin et al 1999). In order to visualize the laryngeal activity *in vivo* under normal articular movements, the fiber optics were inserted into the lower pharynx via nasal cavity (Sawashima 1977). The ultrasonography of the larynx would provide further details of the VF cartilaginous and endolaryngeal structures. Unfortunately the works were successful only in infants and children (Garel et al. 1990; Friedman 1997), and the B-mode US images for adult true VF and vocal muscles which appear as hypoechoic structures were often inconclusive (Raghavendra et al. 1987). Nevertheless, vocal cord paralysis that alters the symmetry of VF vibrations can be easily identified using echoglottography (Schindler et al. 1990; Ooi et al. 1995; Friedman 1997).

The motion of the VF is very complex during phonation. Hirano (1974) proposed a body-cover mechanical model to simulate multi-layered VF structures

(Fig. 1). In which two upper and lower masses of the “cover” (representing the epithelium and the superficial layer of the lamina propria) that interconnected with a spring were coupled laterally to the “body” mass (the vocal muscle and ligament) by springs and viscous dampers (Ishizaka and Matsudaira 1972). The “body” mass was further linked laterally to the thyroid cartilage using a spring and a damping element. During phonation the contractions of the CT and TA muscles effectively alter the tensions acting on the “body” and “cover” tissues (Story et al. 1995). Since the cover is the main vibratory element of the VF, the mechanical properties of the mucosa and the aerodynamic forces acting on the VF play important roles in the formation of voice.

Direct measurement of the stiffness of human VF during normal phonation is extremely difficult, since the measurement devices or markers in contact with the VF is necessary (Isshiki et al. 1985; Berke 1992; Berke and Smith 1992; Tran et al. 1993). However, for an elastic medium, the wave propagation velocity (c) is directly correlated with the intrinsic tension force (T) and inversely proportional to its mass length-density (μ) (Achenbach 1984; Fetter and Walecka 1986).

$$c = \sqrt{\frac{T}{\mu}} \qquad (1)$$

For a given tissue displacement, the tension (T) is proportional to the stiffness or elastic modulus of the medium. This provides an alternative way of estimating soft tissue stiffness noninvasively. Both extrinsic longitudinal tension of the VF cover and the internal stiffening of the VF body would contribute to the change in overall VF stiffness. Due to the sinusoidal nature of mucosal wave, the VF displacement, $y(x, t)$, can be approximated by (Nasri et al. 1994)

$$y(x, t) = A_o \cos [2\pi(x-ct)/\lambda] \quad (2)$$

where A_o is the maximum amplitude of the horizontal displacement (Fig. 1), c is the mucosal wave velocity (MWV) that traveling vertically, and λ is the wavelength. The horizontal displacement velocity (HDV) can be derived from the time rate of change of mucosal geometry, $\partial y(x, t)/\partial t$:

$$v = \partial y(x, t)/\partial t = 2\pi A_o (c/\lambda) \sin [2\pi(x-ct)/\lambda] \quad (3)$$

Apparently, the magnitude of the HDV (v) of the VF is linearly proportional to the MWV (c). The HDV that determined from the displacement of the upper edge of the VF can be measured optically without touching the VF. Therefore, recent laryngeal researches for the mechanical properties of the VF have been focused on the measurements of mucosal wave propagation (Tanaka and Hirano 1990; Sloan et al. 1993; Titze et al. 1993; Nasri et al. 1994; Hanson et al. 1995). In which the phase differences between the strobe marks on the vibrating VF were measured to derive the MWV in canine or human larynges.

The VF that vibrates typically at a fundamental frequency up to a few hundred Hertz poses a great challenge to the US imaging system. However, the US causes the least interference to the VF during normal phonation, it will be the most promising *in vivo* tools for routine laryngeal examination if the interpretation of VF characteristics can be improved quantitatively. In our preliminary US study of the VF functions, we measured the HDV of the VF cover using color Doppler imaging (CDI) and correlated it with the stiffness of the mucosa (Hsiao et al. 2001). The aim of this study was to develop a novel technique that quantify the human MWV directly and non-invasively using commercially available color duplex US system. Based on the fundamental physics of a travelling wave, the wave velocity is simply

the product of fundamental frequency and wavelength ($c = f \lambda$). The phonation frequency can be measured easily with a microphone and a spectrum analyzer, and the MVW (c) can be found if one can resolve the wavelength (λ) for the vertical movement of the VF cover. Therefore, our study was focused on how the CDI visualized the vibratory movements of soft tissues and how to use the CDI artifact to measure the mucosal traveling wave. Both *in vitro* phantom validation and *in vivo* VF measurements using CDI have been performed to demonstrate the current methodology.

MATERIALS AND METHODS

The study was performed with a commercially available, high resolution US scanner (HDI-5000, ATL, Bothell, WA, USA) with a 5-12 MHz linear array transducer (L12-5 38 mm, ATL). The CDI frame rate (f_s) of the US system that typically of a few Hertz is much too slow to capture the movement of the VF in real time. The CDI of VF exhibited strobe motion artifacts that generated by the vibratory movements of the VF cover–air interface, and the artifact patterns changed systemically with the intensity and frequency of the voice.

In vitro study of vibrating string

In order to understand the driving mechanism of CDI artifacts and to make a quantitative measurement of the MWV, a phantom was built to simulate the VF with a prescribed vibrating frequency (f) and with a known traveling wave velocity (TWV). The phantom consisted of a vibrating motor capable of delivering vibrating frequency ranges from 50 to 235 Hz under voltage supply of 1.2 to 4.5V and a rubber string of mass length density (μ) of about 0.026 g/cm (Fig. 2). The tension of the string (T) was adjusted by changing the weight (W) that connected to the string via a pulley. With one end connected to the vibrating motor, the other end of the string was secured with a locking screw. The cross-sectional area of the rubber string is about 2.25 mm^2 and the length (L) can be varied from 2 cm to 15 cm. In some cases, we added additional mass on the string to simulate VF polyp or stiffened spots and then observed the differences in CDI.

The vibrating string was immersed in a water container at about 6-7 cm above the bottom surface to reduce the interference of US reflection, and the US

transducer was placed at about 2-3 cm above the string. Furthermore, to see the effects of CDI frame rate on the color artifact, we selected different CDI line-density settings, which allowed us to visualize the string vibration at the frame rates (f_s) with the range from 5 to 7 Hz.

The TWV (c) was measured by using a pair of low-cost U-shape slotted photo interrupters (PTIR-902, Team House Ltd., Taipei, Taiwan) that consisting of a light-emitting diode (LED) and a phototransistor. The string was positioned to obstruct the light of the LED and cast a shadow on the surface of the phototransistor. Within a range of about 1.5mm displacement, the output voltage of the phototransistor varied from 0 to 3V and was linearly proportional to the position of the string. Therefore, no instrumental amplifier was needed. During the vibratory movement of string, the sinusoidal output signals of the two optical sensors were monitored simultaneously on a four-channel digital oscilloscope (TDS-224, Tektronix, Wilsonville, OR). The TWV (c) was calculated based on the separation distance (Δx) of the two optical sensors and the time delay (Δt) of the traveling wave. The photo sensor used in this study was capable of measuring a displacement of 10 μm at a time resolution of 10 μs.

Since the phantom was designed to simulate the VF vibration and to study the physical mechanism of CDI artifacts, two types of driving forces were applied to the vibrating string: (a) Phantom mode A: string vibration generated by a vibrating motor with variable amplitudes on one end. Since the tension of the string was proportional to the motor power that increased with the vibrating frequency, the TWV (c) also increased with the frequency. (b) Phantom mode B: string vibration

generated by a vibrating motor with fixed amplitude on one end. In this case, the string was constrained to move up and down with constant amplitude of about 2 mm at a length of L=12cm. Therefore, the tension of the string and the TWV (c) were kept constant at various vibrating frequencies.

In vivo study

A total of 10 healthy adult volunteers (6 men and 4 women) aged 34±5 with normal VF function were recruited for this study. Each gave informed consent to take part in the experiments. Ultrasound examination was performed with the subjects in sitting position (Fig. 3). Movements of the VF were monitored in prolonged phonation of various pitches. The voice signal was detected with a precision microphone (ECM-672, SONY, Tokyo, Japan) and the fundamental frequency (f) was measured and displayed on the digital oscilloscope (TDS-224) that equipped with fast Fourier transform (FFT) module (TDS2MM). To verify the difference in fundamental frequencies given by the voice and the VF, an accelerometer (AS-50B, Kyowa, Tokyo, Japan) in some cases was simultaneously attached to the larynx to measure the VF vibration directly.

The sound level of the voice was measured with a precision sound level meter (Type 2235, Brüel & Kjær, Nærum, Denmark) that placed in front of the subject at a distance of about 30 cm away from the mouth. By using “A” frequency weighting and “Random” sound incidence settings in the sound level meter, the subjects were asked to keep the sustained vowel at a sound level of about 65-75 dB for males and 70-80 dB for females.

To measure the mucosal wave propagation, a correct positioning of the US transducer is obtained if the US scanning plane gives a coronal view of the vocal cord. The US transducer was placed vertically at about anterior one-fourth of the thyroid cartilage lamina (Fig. 4a), which was at the mid-portion of antero-posterior VF dimension where the VF vibrated at the maximal excursion (Isshiki 1989). By using color Doppler imaging, the mean velocity (HDV) of tissue displacement in the VF cover area can be measured (Figs. 4b, 4c). The red-blue color of CDI artifact signifies the strobe-motion of the vibratory VF toward and away from the US transducer respectively.

For each measurement, the VF structure was first observed with a scanning window of width of 3.8 cm and depth of up to 4 cm. The B-mode frame rate was typically about 25 Hz. For a sinusoidal VF vibration, the mean velocity toward the US transducer (CDI red code) is the same as that away from the transducer (CDI blue code). In the color mode, to obtain a better CDI velocity resolution in the higher range, the measuring velocity scale was set to the maximum (0 to 128.3cm/s) with the baseline offset. The CDI artifact wavelength (λ_{CDI}) was given by the interval of a pair of bright-dark strip (Fig. 6a). In most of the cases, a scanning depth of 4 cm was high enough to detect the vibratory part of the VF. The corresponding pulse repetition frequency (PRF) was 10000 Hz, and the CDI frame rate (f_s) was about 6 Hz typically. Two female patients who suffered from phonation disorder (unilateral VF polyp) were also included in this study.

RESULTS

Figure 5 depicts the TWV (c) measured for a rubber string (phantom mode A) that vibrates at various frequencies. The TWV of the string was linearly proportional to the vibrating frequency since higher driving force was given. Figures 6a-6d show the results of CDI for such a string that vibrates at frequencies of f = 57, 119, 161 and 204 Hz respectively under variable tensile forces. The vibratory movements of the string caused artifact strips underneath the string in a regular fashion. The locations where small plastic tapes were attached (arrows) generated strong artifact reflections.

The wavelengths of the artifact strips (λ_{CDI}) that measured directly from the CDI and the corresponding TWV(c) measured by the photo sensors are listed in Table 1. It is obviously that the CDI wavelength (λ_{CDI}) decreases with the increase in vibrating frequency (f). Moreover, the CDI frame rate (f_S) also played an important role on the generation of vibratory artifacts. Figure 7 shows the CDI of a string vibrates at f = 57 Hz while the frame rates (f_S) were altered from 5 to 7 Hz. The strings appeared in gray-color wavy shape and had about the same amplitudes under different CDI frame rates (f_S), but the string wavelengths observed increased with f_S. The color artifacts under the string correlated directly with the strobe waveform of the string. Apparently, the CDI artifact wavelength (λ_{CDI}) correlated positively with the frame rate (f_S). Since the TWV (c) is known (406 cm/s), we find the ratio of true wavelength (λ) to the CDI wavelength (λ_{CDI}) can be factorized as a function of the frequency ratio, (f /f_S).

For the phantom mode B, the typical results of CDI for a string that vibrating with fixed TWV (i.e., c=938 and 1470 cm/s) were listed in Table 2. Again the CDI artifact wavelengths (λ_{CDI}) were found correlate strongly with the frequency ratio (f/f_s). After the extensive tests by varying the length (L) and tension (T) of the string and taking all the parameters into account, we found that the CDI artifact wavelength (λ_{CDI}) can be factorized into a simple relationship that

$$\lambda_{CDI} \cong (3.94 \pm 0.17) \cdot (f_s / f) \quad \text{(cm)} \qquad (4)$$

Figures 8a and 8b show the typical coronal-views of VF CDI for a male subject that phonating at a fundamental frequency of 112 Hz with different sound pressure levels, SPL=65dB and 80dB, respectively. Although the detail VF structure could not be seen clearly, the mucosal waves that traveling vertically generated an “Africa” like color artifact underneath the VF-airspace interface. The VF “body” (vocal muscle and ligament) appeared in gray-color embedded in the CDI motion artifact. The fundamental frequency of the voice recorded by the microphone was found identical to that measured with the accelerometer. When the voice ceased, the color signals disappeared immediately. The CDI vibratory artifact patterns became irregular when the SPL was too high which might also cause the saturation artifact of Doppler color.

During sustained phonation, the vibratory movement of the mucosa generated the color artifact that extended vertically. Since both upper and lower margins of the VF were stationary, the horizontal width of the vibratory artifact should correspond to half of the mucosal wavelength (λ). Using the C++ image processing software that developed earlier (Shau et al. 1999), we measured the

horizontal width (L_m) of the CDI color artifact under the VF for each US image (Fig. 8a) and took the average value typically for over 5-7 sequential frames. Based on the model of finite string with fixed endpoints, the mean mucosal wavelength is simply given by $\lambda=2\ L_m$. Therefore, we can use it to calculate the mean MWV (c) directly based on the fundamental frequency (f) that indicated by the spectrum analyzer, $c= f\ \lambda$. Figures 9a and 9b depict the results of MWV measured for the male and female subjects respectively. In the sustained phonation in their comfortable pitch and soft-intensity, the mean MWVs for the males vary from 2.1 to 10 m/s in frequency range of 85-310 Hz, the females have MWVs that vary from 5.0 to 16.5 m/s in frequency range of 180-480 Hz. Female subjects typically phonated at a higher fundamental frequency, and the corresponding SPL is also higher. Therefore, the VF CDI vibratory artifacts for the female subjects were much more irregular than that of the male subjects due to higher SPL (as in Fig. 8b). The uncertainty in the MWV measurement was typically below 5% and the results were very repeatable.

Figure 10 shows the typical VF CDI for a female patient with polyp, the color artifacts are more irregular than that of normal phonation. With a hoarse voice, the motion of the VF with polyp caused asymmetric artifacts as the mucosal waves propagated upward vertically. From the color codes, we found the subglottic mucosal wave with higher vibratory movement (on the right) was severely dampened as it moved across the polyp (to the left) and the “Africa” artifact pattern was altered.

DISCUSSIONS

Quantitative assessment of the VF function accurately is the goal that voice clinicians have long searched for. To meet the requirements for routine laryngeal examination, the method must be easy to perform and analyze, cost effective, and with a minimum disturbance to the voice production. The medical ultrasound seems to be one of the best choices if the basic phenomena of sonography for the vibratory VF can be well understood.

Color Doppler ultrasound Imaging has been used extensively as a non-invasive tool for quantifying blood flows, however, little is known about its application on detecting high-frequency vibratory movements. Generally, medical ultrasounds that used clinically were inadequate to visualize the vibratory movement of the VF due to the limits in frame rate and spatial resolution. Although the A-M mode echoglottography may provide a better time-resolution, the complexity of the changes in VF shape during phonation creates very confusing echoes (Hertz et al. 1970; Holmer et al. 1973; Hamlet et al. 1980; Miles 1989). Ooi et al. (1995) first used the CDI to identify vocal cord palsy based on the asymmetry of color flow patterns, but the CDI vibratory artifacts was somewhat mis-interpreted.

The vibrating frequency, amplitude, the mass density and the acoustic impedance of the soft tissues were found to play important roles in the formation of US color artifacts. At a given CDI frame rate (f_s) the US system scanned through the region-of-interest line-by-line sequentially, thus for a finite string that vibrated at a frequency (f) higher than f_s the string would appear in sinusoidal waveforms.

The colored artifact strips were generated accordingly and the local color indicated the mean movement velocity and direction of the string at the time of Doppler sampling. Therefore, the wavelength of the color strips (λ_{CDI}) in CDI reflected the frequency of the vibratory motion relative to the US frame rate (f/f_S). The constant, 3.94, in eqn (4), was related to the equivalent line-scanning velocity (i.e., $3.94f_S$ cm/s) for the present CDI system setting.

As shown in Fig. 6a, we attached small plastic tapes on the surface of the rubber string to simulated the hardened spot on the VF, the strong color artifacts were observed to reflect from the sites of the tapes due to higher difference in acoustic impedance. For a small vibratory movement of uniform rubber string, the penetration depth of the color artifact is proportional to its velocity. It should be noted that the Doppler frequency aliasing might occur if the vibrating velocity exceeded the PRF's Nyquist limit. The CDI frame rate may be responsible for the spatial aliasing; a lower PRF or Doppler velocity scale may result in frequency alasing.

The CDI of the VF movement during sustained phonation exhibited similar color artifacts as of the vibrating string (Figs. 4b, 4c), and the color artifacts were originated from the mucosal cover and air interface where acoustic discontinuity was encountered. In coronal view of the VF, the cover moved medio-laterally in the direction toward and away from the US transducer, and the color of the CDI artifacts represents the mean velocity of the vibrating mucosa. The vibrating frequency (f) predicted from the wavelength of color strips (λ_{CDI}) agrees with the fundamental frequencies of both the voice recorded by microphone and the

laryngeal vibration that detected by accelerometer. Noted that the vibratory movement of complex VF structure resulted different HDVs along the mucosal surface vertically, however, the VF cover vibrated as a finite membrane with fixed ends since the artifact wavelengths (λ_{CDI}) along the mucosa were about the same. The width of the color artifacts in VF coronal view indicates the vertical extent that VF vibrates during phonation.

Although it has been well known that the “stiffness” of the VF greatly affect its vibratory movement in phonation, *in vivo* studies of human VF mechanical properties have been limited (Isshiki et al. 1985; Berke and Smith 1992). The measurements were invasive and were made during laryngeal surgery. Non-invasive measurements of human VF stiffness were focussed on the propagation of mucosal wave that observed from the oral side (Sercarz et al. 1992; Hanson et al. 1995). During voicing the mucosal wave was observed to propagate upward from the mucosal upheaval (Yumoto et al. 1996).

Unlike the lateral length scale of the vocal cords that is identifiable with laryngostroboscopy, the vertical dimension of the VF during phonation cannot be seen easily since there is no natural landmarks available. However, using CDI the vertical length scale of the vibrating part of mucosa can be visualized from the color artifacts (Fig. 8a), which leads to the mean MVW (*c*). As indicated in our *in vitro* study, the penetration depth of the color artifact was proportional to the movement velocity locally, thus the “Africa” shape of the color artifact revealed the spanwise variation of MWV during glottal cycle.

The mean MWVs for the male subjects were found vary from 2.1 to 10 m/s in frequency range of 85-310 Hz at their comfortable pitch and SPL, the results agreed with those reported in literature (Tran et al. 1993; Hanson et al. 1995). The females typically had higher MWV that varied from 5.0 to 16.5 m/s in frequency range of 180-480 Hz. To our best knowledge, this is the first time that effect of gender on the MWV be reported since the edge of mucosal wave is difficult to be seen by laryngostoboscopy in female subjects (Hanson et al. 1995). With the increase in phonation frequency, the SPL for the voice was slightly raised since the threshold pressure increased with the fundamental frequency (Titze 1988). The females typically phonated at a SPL of about 5-10 dB higher than the males for the same vowel, their VF CDI vibratory artifacts were not as regular as those for the male subjects phonating at a soft voice.

For the voice beyond a fundamental frequency of 350 Hz the vibratory HDV of female subjects would exceed the maximum Doppler velocity scale (128 cm/s) and the saturation color artifacts also appeared. The vibratory artifact may lose it uniformity in color strips when the SPL is high or saturation; however, the width of the color artifact that gives the vertical extent of mucosal wave is not affected (Figs. 8a, 8b). Hirano (1974) studied the morphological structure of the VF under different laryngeal adjustments, for a soft voice at low pitch levels both the VF cover and the body were very flexible and equally involved in the vibratory movement. For a loud voice at medium-high pitch level, the VF body increased its stiffness due to stronger contraction of vocalis muscle while the cover maintained it softness. The spotty CDI artifact that appears in high pitch and loud voice may be attributed to the vibratory interaction of the slackened VF cover and

the stiff VF body.

Noted that the VF's stiffness would be different between the transverse and the longitudinal aspects. Comparisons of the changes of MWV for male and female VF showed the same trend with respect to the fundamental frequency (Figs. 9a, 9b). The females typically have shorter vocal cord lengths than the males (Kahane 1978; Titze 1989); therefore their fundamental frequencies of voice for comfortable vowel are also higher. However, under normal phonation function the mechanical properties of the VF cover for both males and females (based on the slope of their MWV versus frequency) are about the same. All the MWV data fall into relatively the same curve and simply related to the phonation frequency.

The human MWV was slightly higher than that of canine (i.e., 0.9-1.6 m/s, Sloan et al. 1992; 0.5-2.0 m/s, Titze et al. 1993; 0.76-2.2 m/s, Nasri et al. 1994) in the frequency range of 100-180 Hz. Although the infraglottic aspect of human VF vibrates in a similar manner as that of the canine, the intrinsic structures of their VF mucosa are very different (Yumoto et al. 1996). The cover of human VF was found to be thinner and stiffer than that of the canine, and the corresponding MWV was expected to be relatively higher.

This study represents the first attempt to measure the MWV *in vivo* using US. The characteristics of the mucosal wave are valuable clinically for evaluating the vocal disorder. The CDI provided an insight of the dynamics of VF membranous structure during phonation. As demonstrated in the present study, the mucosal scars and mass lesions on the VF may result in abnormal TWV and different CDI

vibratory artifacts. With the help of CDI artifacts, the VF location can be easily identified. It is feasible to apply the color artifacts to measure the MWV with a reasonable accuracy and quantify the human laryngeal function non-invasively using a commercially available US system. However, for the clinicians, the proper positioning of US transducer in scanning the vibrating VF may take a little practice since the VF moves in a complex manner and changes its position during different pitch of phonation.

SUMMARY

In the effort to develop a non-invasive method for evaluating VF functions clinically, we identified the US CDI as a promising technique since it is simple, painless, with the least interference to the phonation path and no need for anesthesia. By tracing the color artifacts generated at the mucosa-air interface, the location of the VF can be easily found with US. The mechanism for the formation of vibratory color artifacts and their correlation with the vibrating tissues were demonstrated with string phantoms. The mean MWV was calculated based on the vibration of a finite string model with fixed ends, and the variation in MWV as it propagated vertically were revealed by the color and shape of the artifacts. The female subjects had shorter vocal cords than the males. Thus, their MWVs were found to extend from the males' data into higher frequency range. The present method is versatile for the investigation of VF biomechanics in a broad range of frequency for different ages and gender. It is also applicable for the evaluation of phonation function for vocal disorders that alters the vibratory movement of musoca. Th use of CDI artifacts may extend the laryngeal US into a bright future in the routine clinical service.

REFERENCES

Achenbach JD. Wave propagation in elastic solids. Evanston, IL: Elsevier Scientific Publishers, 1984:30-33.

Baken RJ, Orlinkoff RF. Clinical measurement of speech and voice, 2nd ed. Thomson Learning, San Diego: Singular Publishing, 2000:393-451.

Berke GS. Intraoperative measurement of the elastic modulus of the vocal fold. Part 1. Device development. Laryngoscope 1992;102:760-69.

Berke GS, Smith ME. Intraoperative measurement of the elastic modulus of the vocal fold. Part 2. Preliminary results. Laryngoscope 1992;102:770-78.

Fetter AL, Walecka JD. Theoretical mechanics of particles and continua. Singapore: McGraw-Hill, 1980:207-263.

Friedman EM. Role of ultrasound in the assessment of vocal cord function in infants and children. Ann Otol Rhinol Laryngol 1997; 106:199-209.

Garel C, Legrand I, Elmaleh M, Contencin P, Hassan M. Laryngeal ultrasonography in infants and children: anatomical correlation with fetal preparations. Pedia Radiol 1990;20:241-44.

Hanson DG, Jiang J, D'Agostino M, Herzon G. Clinical measurement of mucosal wave velocity using simultaneous photoglottography and laryngostroboscopy. Ann Otol Rhinol Laryngol 1995;104:340-49.

Hamlet SL. Ultrasonic measurement of larynx height and vocal fold vibratory pattern. J Acoust Soc Am 1980; 68:121-26.

Hertz CH, Lindstrom K, Sonesson B. Ultrasonic recording of the vibrating vocal folds. Acta Otolaryngol 1970;69:223-30.

Hirano M. Morphological structure of the vocal cord as a vibrator and its variations. Folia Phoniatr 1974;26:89-94.

Hirano M. Clinical examination of voice. Wien-New York: Springer-Verlag, 1981.

Holmer NG, Kitzing P, Lindstrom K. Echoglottography. Acta Otolaryngol 1973;75:454-63.

Hsiao TY, Wang CL, Chen CN, Hsieh FJ, Shau YW. Noninvasive assessment of laryngeal phonation function using color Doppler ultrasound imaging. Ultrasound Med Biol 2001 (in press)

Ishizaka K, Matsudaira M. Synthesis of voiced sound from a two-mass model of the vocal cords. Bell Syst Tech J 1972;51:1233-1268.

Isshiki N. Phonosurgery. Theory and practice. Tokyo: Springer-Verlag, 1989.

Isshiki N, Ohkawa M, Goto M. Stiffness of the vocal cord in dysphonia – Its assessment and treament. Acta Otolaryngol (Stockh) 1985; Suppl.419: 167-74.

Kahane J. A morphological study of the human prepubertal and pubertal larynx. Am J Anat 1978;151:11-20.

Lin E, Jiang J, Hone S, Hanson DG. Photoglottographic measures in Parkinson;s disease. J Voice 1999;13:25-35.

Miles KA. Ultrasound demonstration of vocal cord movements. British J Radiol 1989;62:871-72.

Nasri S, Sercarz JA, Berke GS. Noninvasive measurement of traveling wave velocity in the canine larynx. Ann Otol Rhinol Laryngol 1994;103:758-66.

Ooi LL, Chan HS, Soo KC. Color Doppler imagiong for vocal cord palsy. Head & Neck 1995;17:20-23.

Raghavendra BN, Horii SC, Reede DL, et al. Sonographic anatomy of the larynx, with particular reference to the vocal cords. J Ultrasound Med 1987;6:225-30.

Sasaki CT, Weaver EM. Physiology of the larynx. Am J Med 1997;103:9s-18s

Sawashima M. Fibreroptic observation of the larynx and other speech organs. In:

Sawashima M and Cooper FS, ed. Dynamic aspects of speech production. Tokyo, Japan: Univ Tokyo Press, 1977:31-46.

Schindler O, Gonella ML, Pisani R. Doppler ultrasound examination of the vibration speed of vocal folds. Folia Phoniatr 1990;42:265-72.

Sercarz JA, Berke GS, Ming Y, Gerratt BR, Natividad M. Videistroboscopy of human vocal fold paralysis. Ann Otol Rhinol Laryngol 1992;101:567-77.

Shau YW, Wang CL, Shieh JY, Hsu TC. Non-invasive assessment of the viscoelasticity of peripheral arteries. Ultrasound Med Biol 1999; 25:1377-88.

Sloan SH, Berke GS, Garratt BR, Kreiman J, Ye M. Determination of vocal fold mucosal wave velocity in an *in vivo* canine model. Laryngoscope 1993;103:947-53.

Story BH, Titze JR. Voice simulation with a body-cover model of the vocal folds. J Acoust Soc Am 1995;97:1249-60.

Tanaka S, Hirano M. Fiberscopic estimation of vocal fold stiffness *in vivo* using the sucking method. Arch Otolaryngol Head Neck Surg 1990;116:721-24.

Titze IR. The physics of small-amplitude oscillation of the vocal folds. J Acoust Soc Am 1988;83:1536-52.

Titze IR. Physiological and acoustic differences between male and female voices. J Acoust Soc Am 1989;85:1699-1707.

Titze IR, Jiang JJ, Hsiao TY. Measurement of mucosal wave propagation and vertical phase difference in vocal fold vibration. Ann Otol Rhinol Laryngol 1993;102:58-63.

Tran QT, Berke GS, Gerratt BR, Kreiman J. Measurement of Young's modulus in the *in vivo* human vocal folds. Ann Otol Rhinol Laryngol 1993;102:584-91.

Yumoto E, Yoshimi K, Toshihiro M. Vocal fold vibration viewed from the tracheal

side in living human beings. Otolaryngol Head Neck Surg 1996;115:329-34.

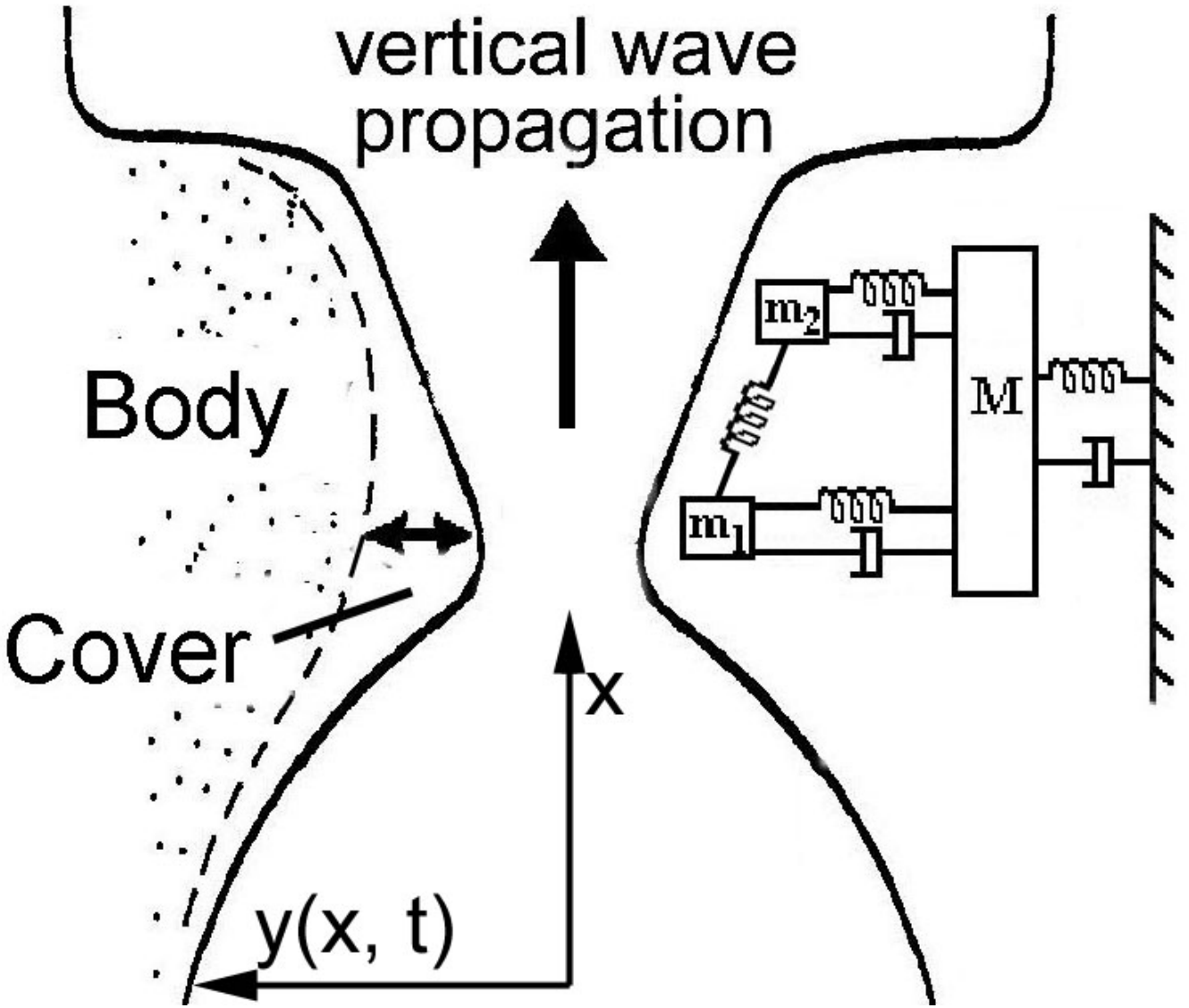
vertical wave
propagation
Body
Cover
x
y(x, t)
m2
M
m1

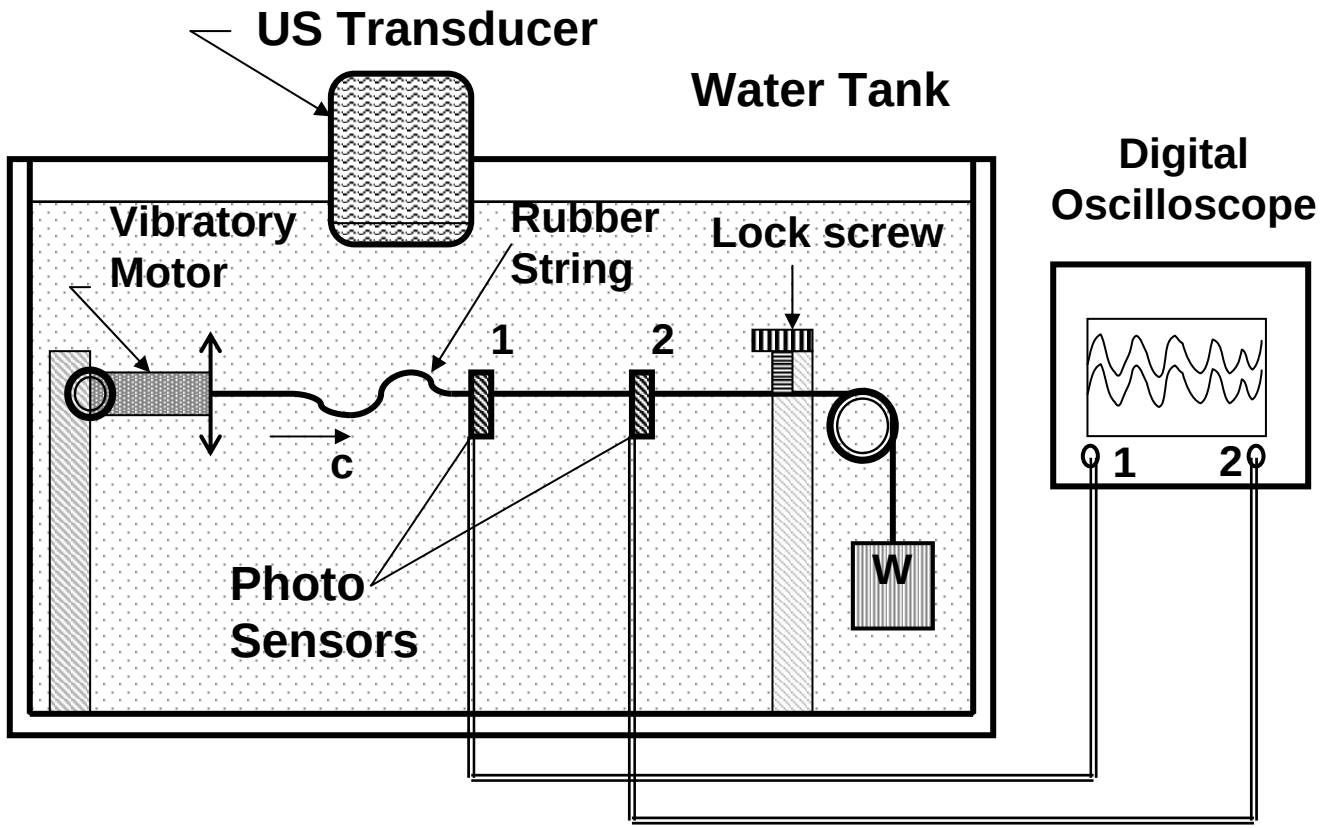
US Transducer
Water Tank
Digital
Oscilloscope
Vibratory
Motor
Rubber
String
Lock screw
1
2
c
W
Photo
Sensors
1
2

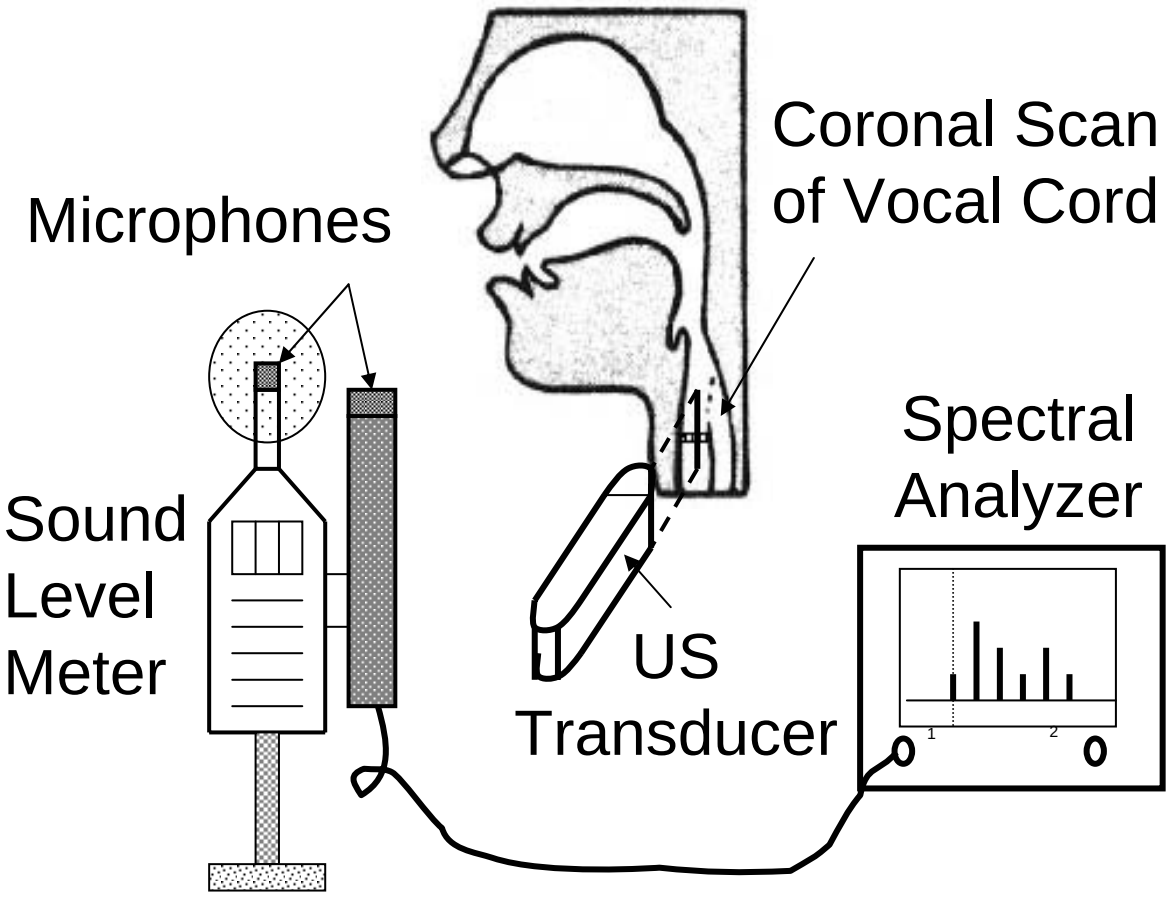
Microphones
Coronal Scan
of Vocal Cord
Sound
Level
Meter
Spectral
Analyzer
US
Transducer
1
2

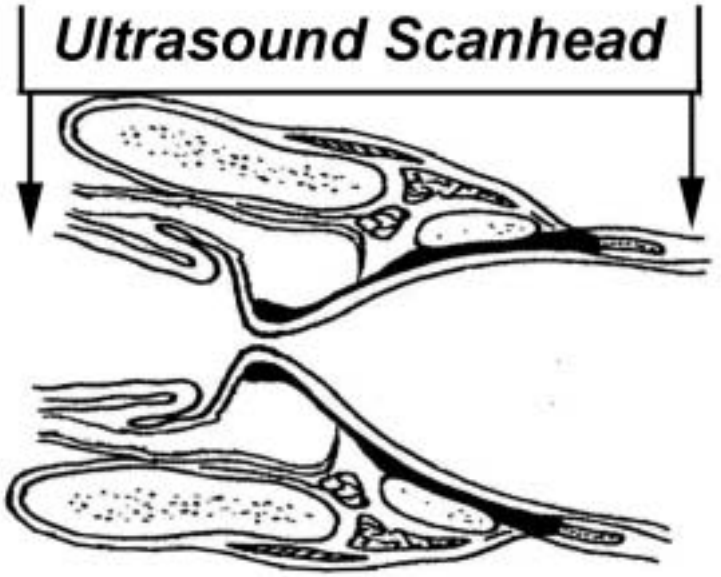
Ultrasound Scanhead

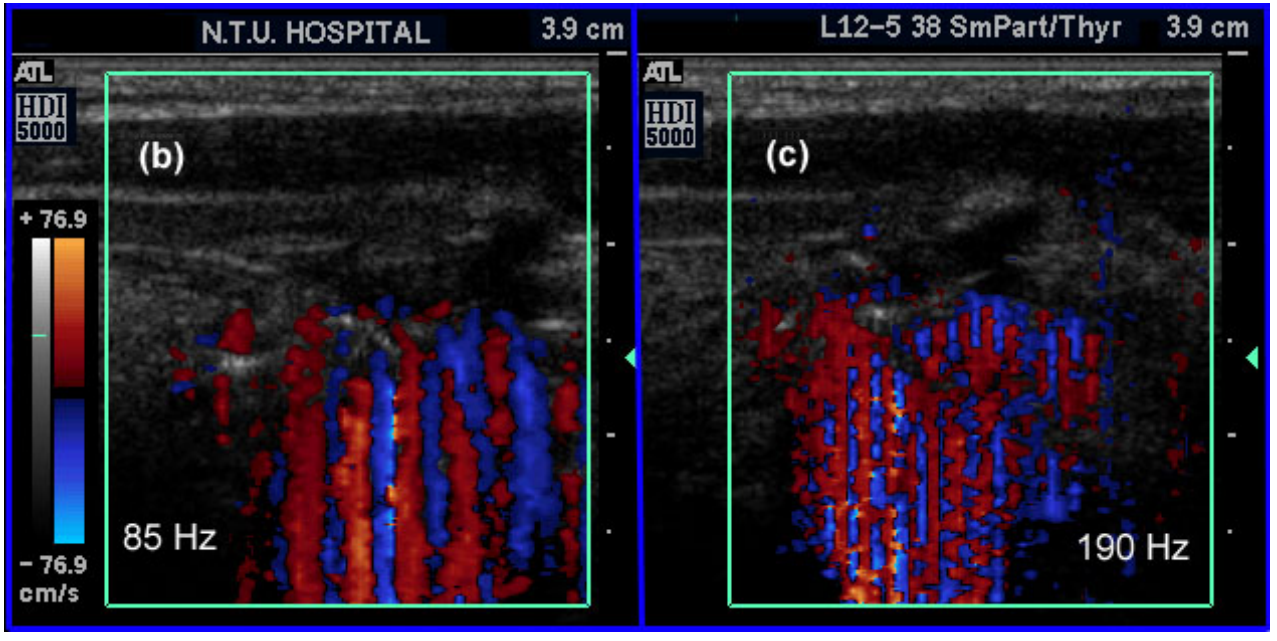
N.T.U. HOSPITAL
3.9 cm
ATL
HDI 5000
(b)
+ 76.9
– 76.9
cm/s
85 Hz
L12-5 38 SmPart/Thyr
3.9 cm
ATL
HDI 5000
(c)
190 Hz

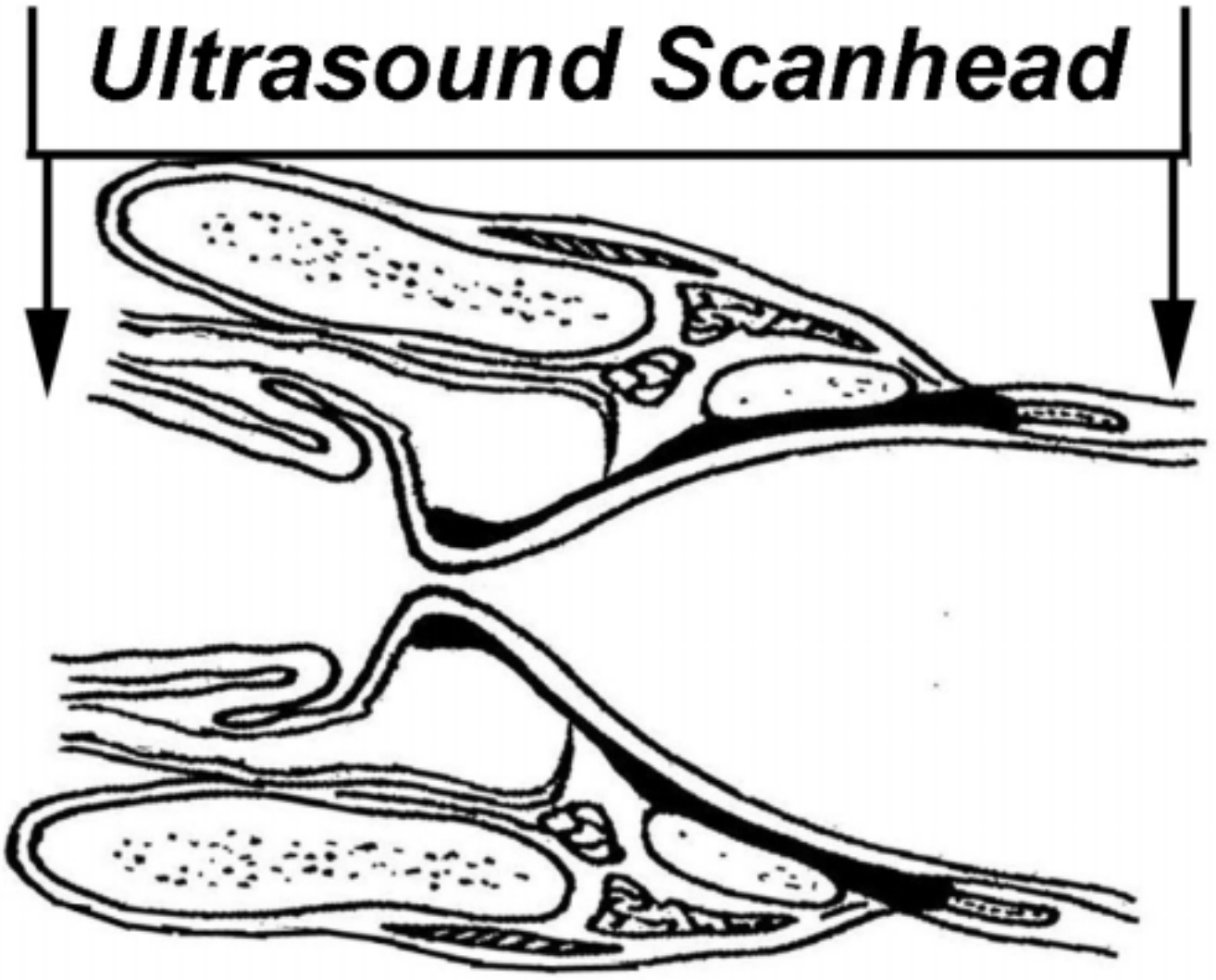
Ultrasound Scanhead

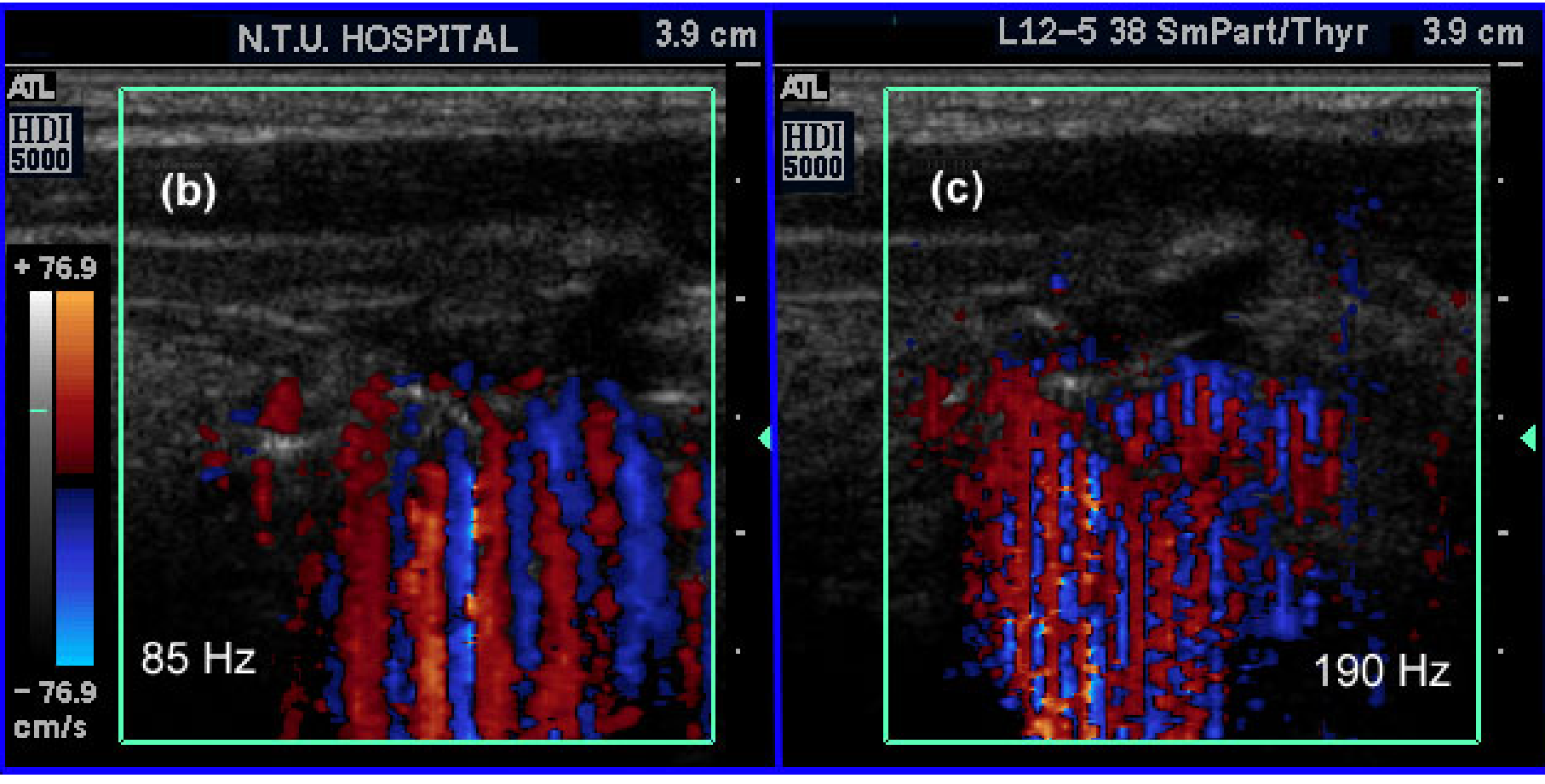
N.T.U. HOSPITAL
3.9 cm
ATL
HDI 5000
(b)
+ 76.9
– 76.9
cm/s
85 Hz
L12-5 38 SmPart/Thyr
3.9 cm
ATL
HDI 5000
(c)
190 Hz

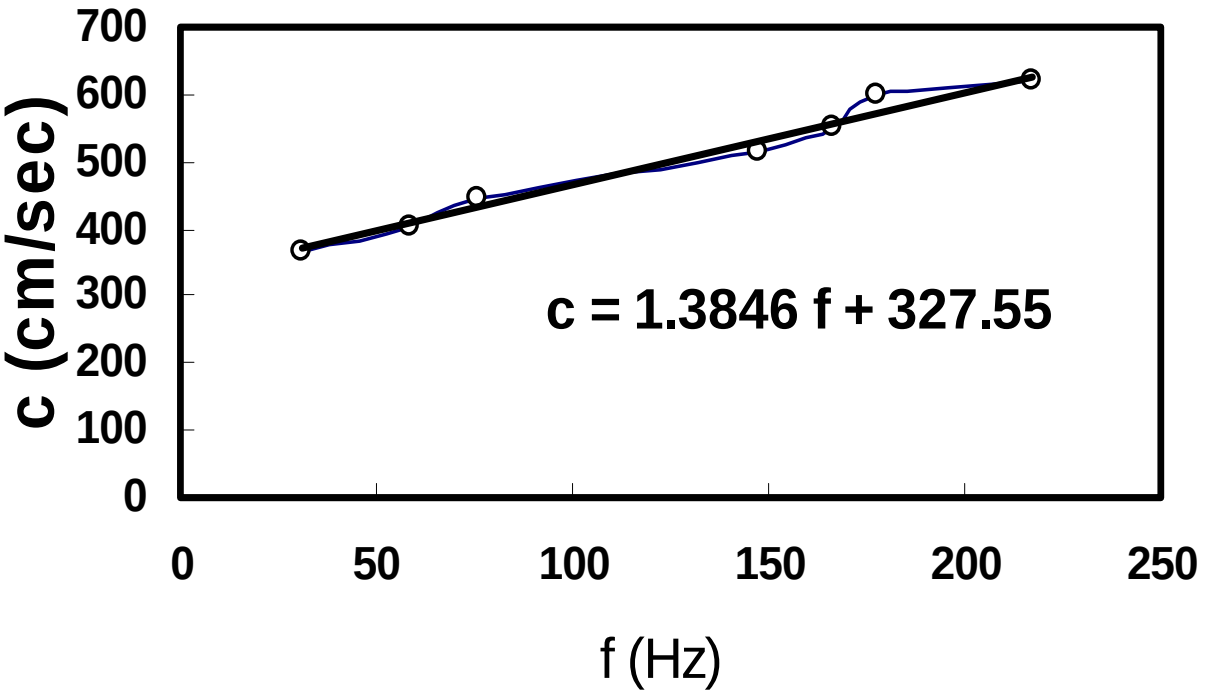
700
600
500
400
300
200
100
0
c (cm/sec)
c = 1.3846 f + 327.55
0
50
100
150
200
250
f (Hz)

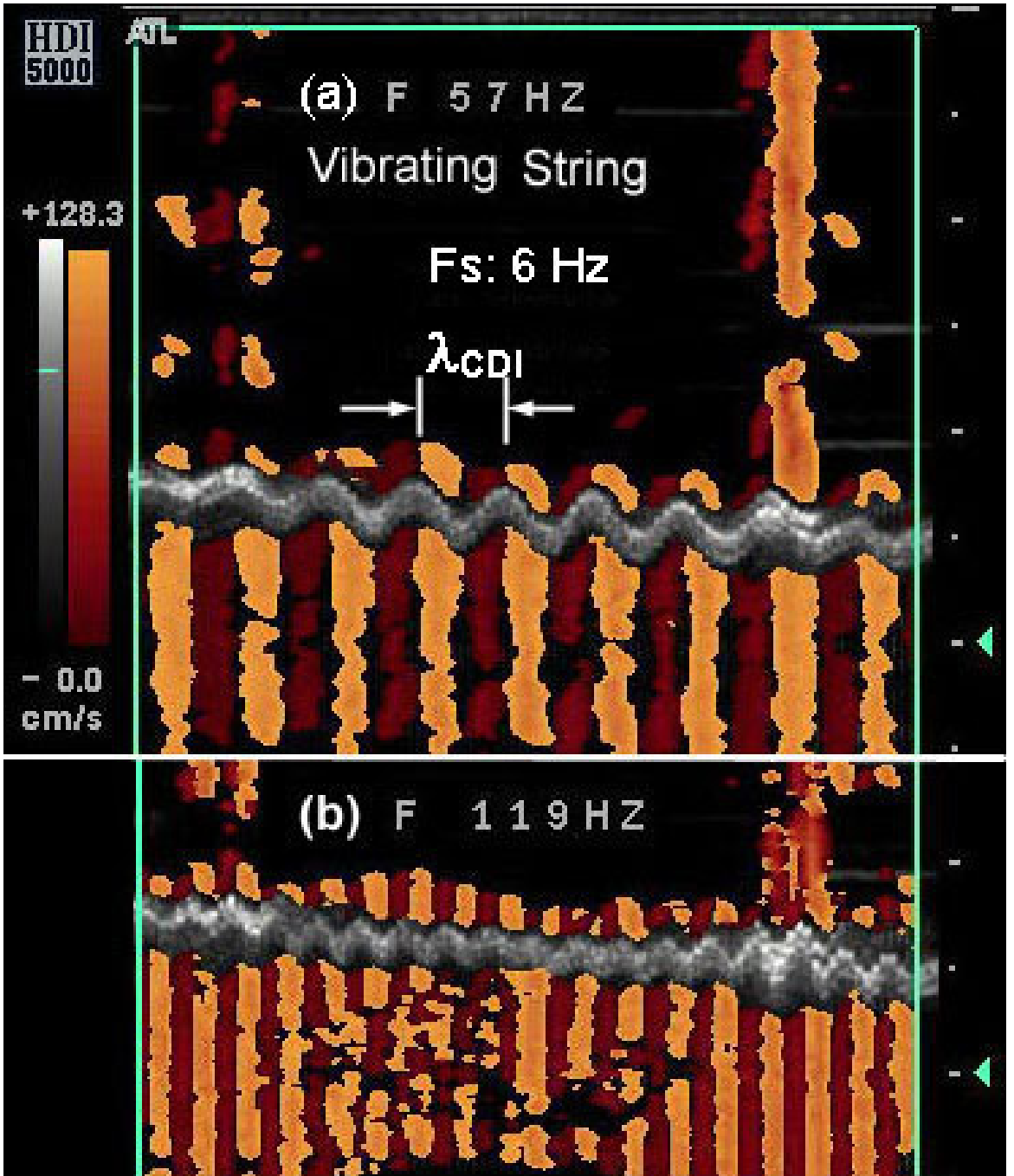
HDI
5000
ATL
(a) F 57 HZ
Vibrating String
+128.3
Fs: 6 Hz
λcDI
– 0.0
cm/s
(b) F 119 HZ

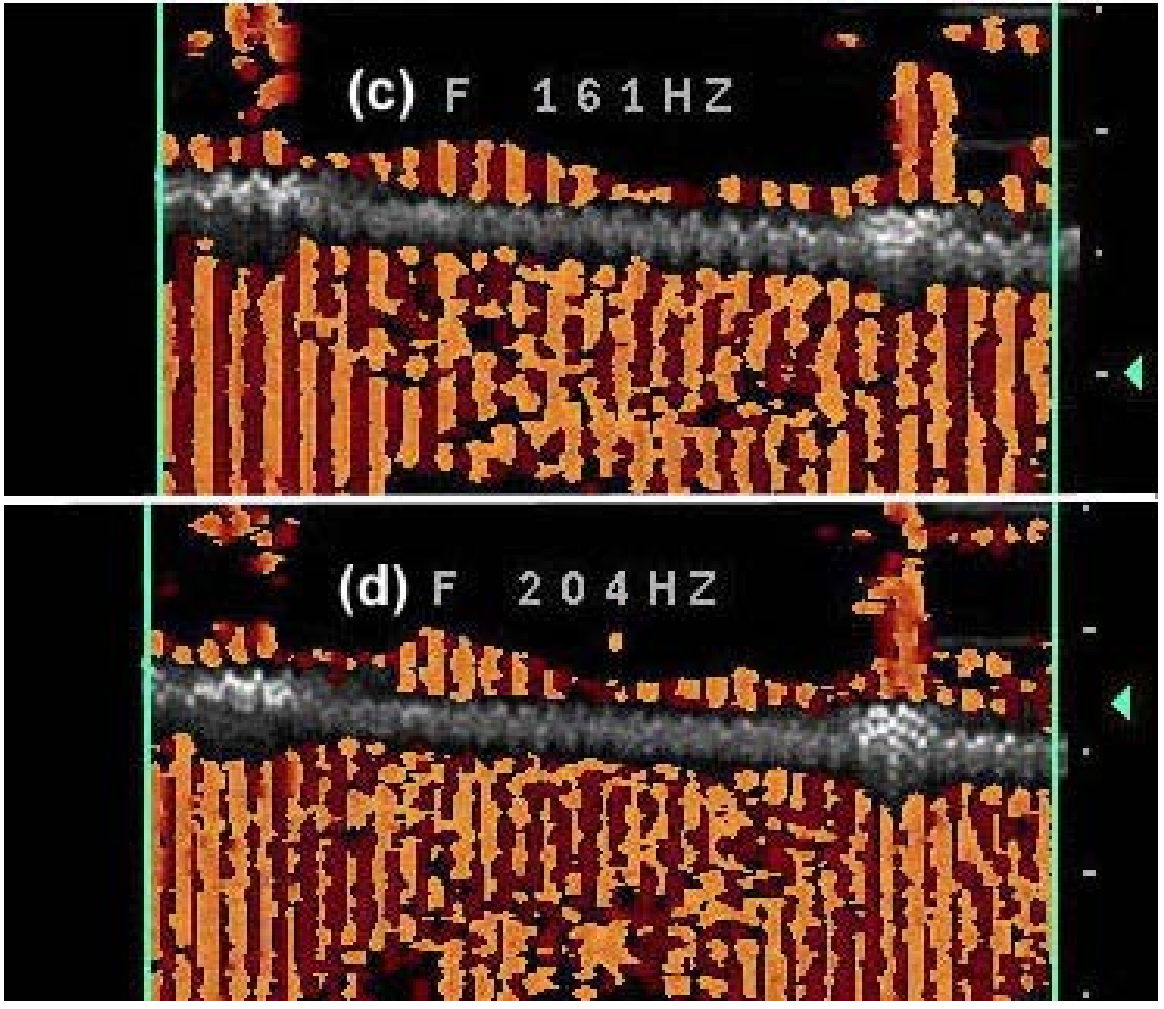
(c) F 161HZ
(d) F 204HZ

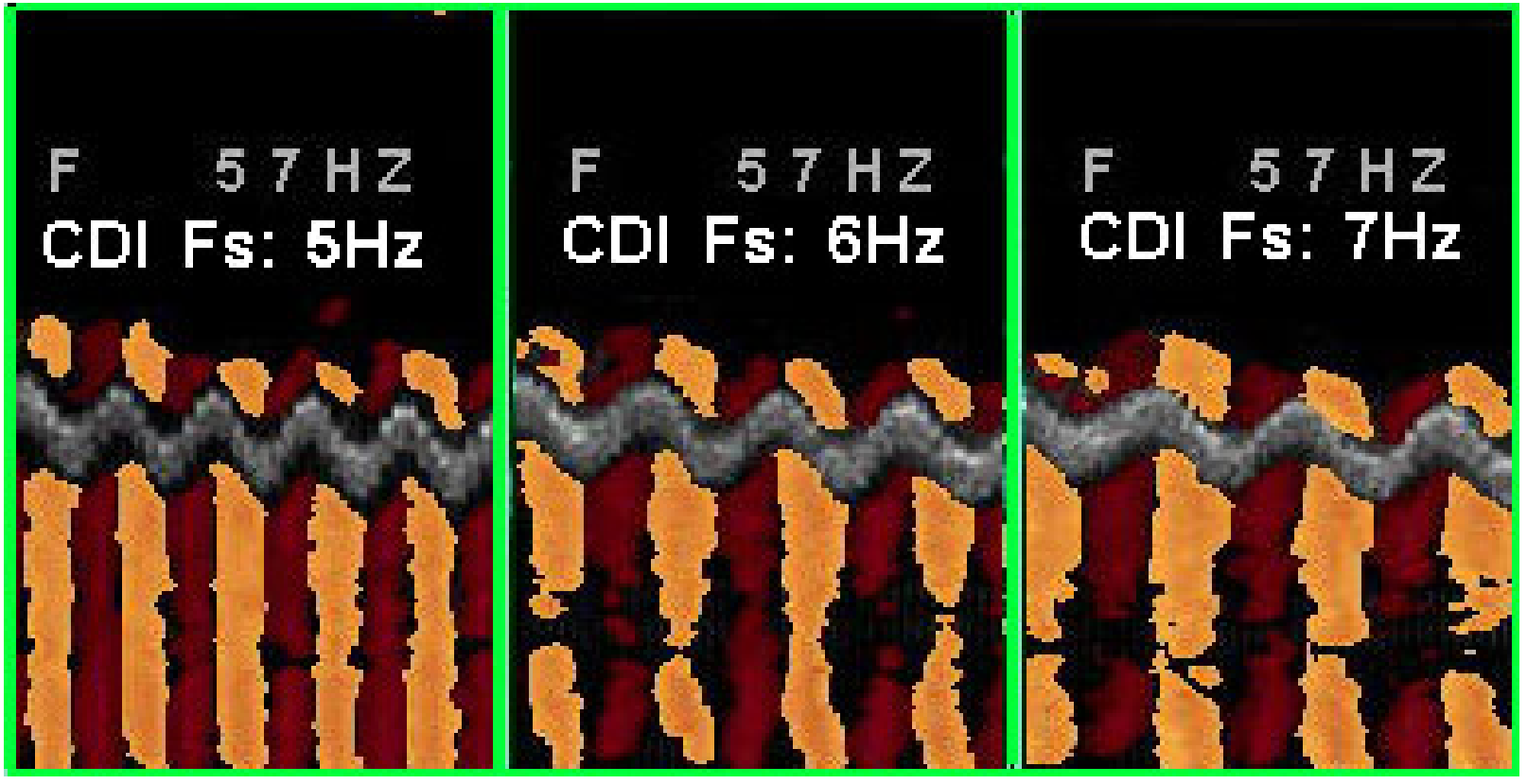
F 57HZ
CDI Fs: 5Hz
F 57HZ
CDI Fs: 6Hz
F 57HZ
CDI Fs: 7Hz

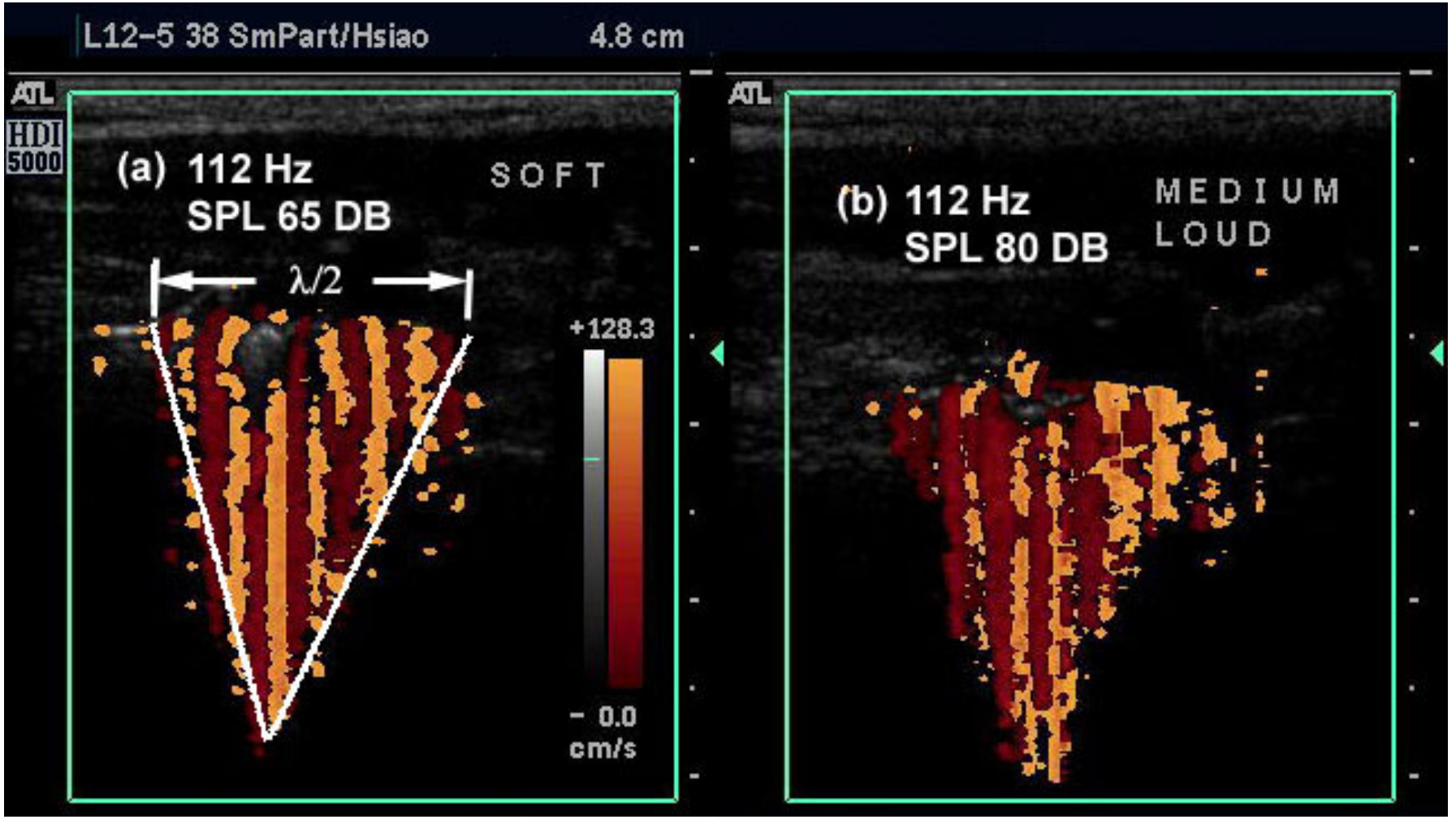
L12-5 38 SmPart/Hsiao
4.8 cm
ATL
HDI 5000
(a) 112 Hz
SPL 65 DB
SOFT
λ/2
+128.3
– 0.0
cm/s
ATL
(b) 112 Hz
SPL 80 DB
MEDIUM
LOUD

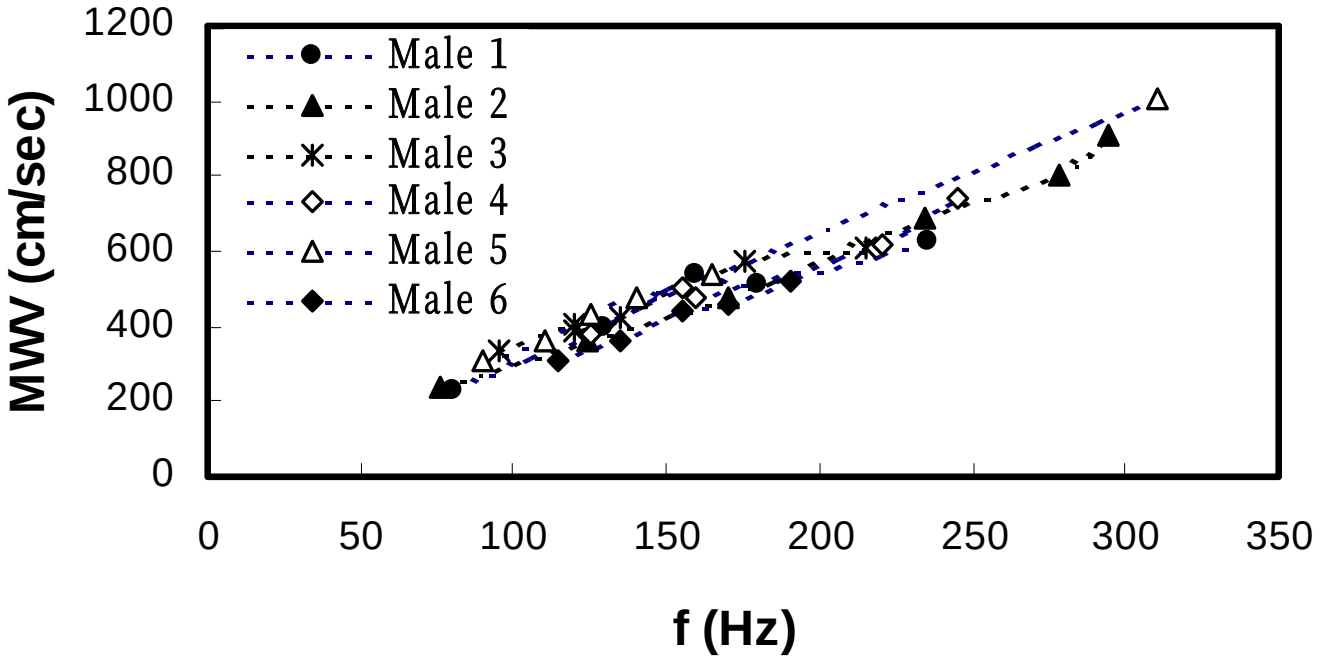
MWV (cm/sec)
1200
1000
800
600
400
200
0
Male 1
Male 2
Male 3
Male 4
Male 5
Male 6
0
50
100
150
200
250
300
350
f (Hz)

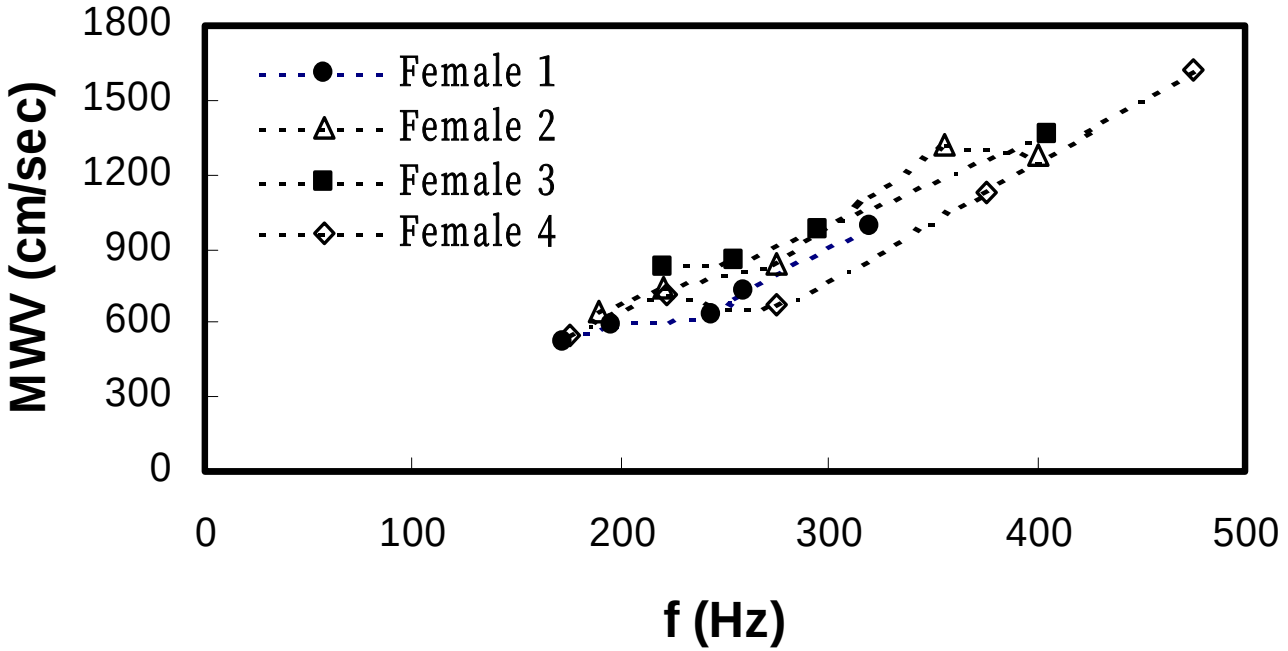
1800
1500
1200
900
600
300
0
MWV (cm/sec)
Female 1
Female 2
Female 3
Female 4
0
100
200
300
400
500
f (Hz)

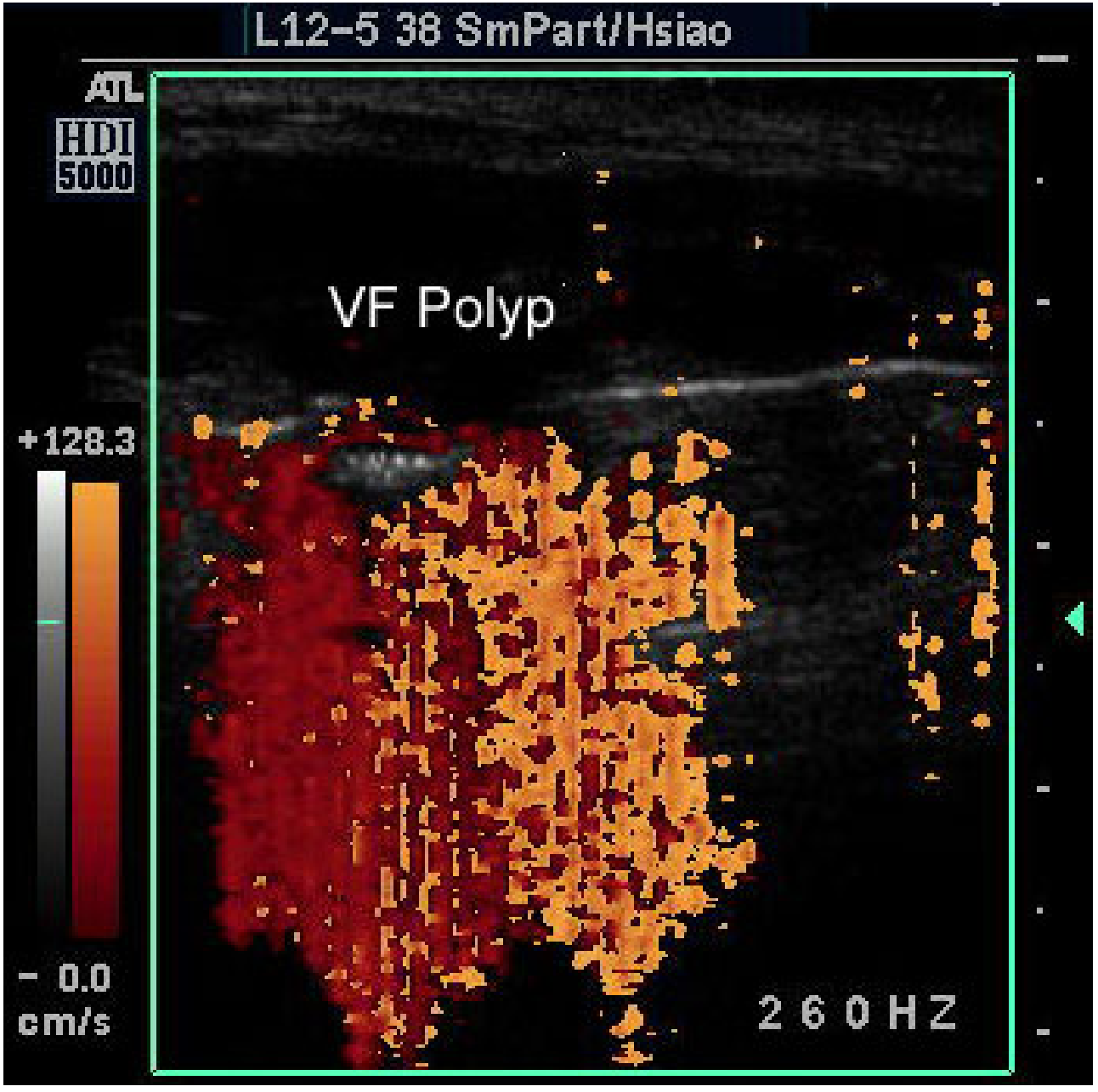
L12-5 38 SmPart/Hsiao
ATL
HDI
5000
VF Polyp
+128.3
- 0.0
cm/s
260HZ